

Morphological and enzymatical characterization of the infection process of *Pythium ultimum* in *Dendrobium officinale* (Orchidaceae)

Yong-Mei XING^a, Xiang-Dong LI^{a,b}, Meng-Meng LIU^a,
Gang ZHANG^c, Chun-Lan WANG^a & Shun-Xing GUO^{a*}

^a*Institute of Medicinal Plant Development, Chinese Academy
of Medical Sciences & Peking Union Medical College, Malianwa North Road 151,
Beijing 100193, P. R. China; e-mail: sxguo1986@163.com*

^b*China National Corporation of Traditional and Herbal Medicine
e-mail: cell2008@126.com*

^c*College of Pharmacy, Shaanxi University of Chinese Medicine,
Xi'an, 712046, China
e-mail: Zhang_jay_gumling2003@aliyun.com*

Abstract – Observations of the ultrastructural morphology of leaf segments of *D. officinale* with or without *P. ultimum* infection were made using light microscopy, scanning electron microscopy and transmission electron microscopy. FITC labelling was used to mark cellulose before and after infection by the pathogenic fungus, and observations were performed with a confocal laser-scanning microscope. The results showed that after infection by *P. ultimum*, the mycelia pierced the leaf tissue of *D. officinale* through the stomata of the guard cells gradually and changed into structures resembling penetration pegs under microscopy and SEM observations. The appressorium was observed to adhere to the stoma. Furthermore, the fluorescence intensity of cellulose labelled with FITC was much lower in *D. officinale* leaves infected by *P. ultimum* than in healthy leaves. Soft rot disease in *D. officinale* infection with *P. ultimum* might be related to direct penetration into the cell walls of the plant and the cellulases secreted by the pathogen, which partly contributed to step-by-step degradation of the cell walls of the host plant.

Cellulose-FITC / Scanning electron microscopy / Semi-thin microtomy / Transmission electron microscopy / Soft rot disease

INTRODUCTION

Dendrobium officinale is an Orchidaceae family plant that is considered as a Chinese medical herb (Xing *et al.*, 2011). It is listed in the Pharmacopoeia of the People's Republic of China because of the special pharmacological significance of its stems, which are used in the treatment of gastritis and cancer (Zhang *et al.*,

* Author to whom correspondence should be addressed.
Yong-Mei Xing and Xiang-Dong Li contributed equally to this work.

2012). However, wild populations of *D. officinale* have been severely depleted due to inefficient protection and overharvesting. Thus, large-scale artificial cultivation using tissue culture to supplement the sources of this plant in the field has attracted serious attention from researchers in China. Because *Dendrobium* species prefer to grow under mild and moist conditions, severe pathogenic oomycete diseases are inevitable. These diseases hamper the production of *D. officinale*. In addition, *Pythium vexans* has been reported to cause stem rot in certain species, e.g., *D. chrysotoxum*, *D. thyrsoflorum* and *D. aurantiacum*, in Yunnan Province, China (Tao *et al.*, 2011).

In the previous studies by our laboratory, a pathogenicity test was performed on oomycete-infected *D. officinale* in the greenhouse and in the field according to Koch's postulates. The pathogenic oomycete was identified with morphological and molecular biological analysis as *P. ultimum* (Li *et al.*, 2011). According to the previous studies, *P. ultimum* infects tender and juicy buds, as well as new branches. Subsequently, the pathogenic oomycete causes root, flower and leaf rot and soft rot of the seedlings and ultimately results in the prompt death of the plant (Li *et al.*, 2013).

Cellulose, a complex carbohydrate, is the basic structural component of plant cell walls and is mainly composed of long polymers of β 1-4, linked glucose units (Somerville, 2006). Endo- β -(1-4)-D-glucanase, exo- β -(1-4)-D-glucanase and β -glucosidase, the three major enzyme components of cellulase enzyme complex, work synergically in plant cellulose degradation (Kim *et al.*, 2008). Phytopathogenic fungi produce three major cellulases: endoglucanase, exoglucanase and cellobiase (Klyosov, 1990). As is well documented, a fluorescence technique for *in situ* staining of cellulose with fluorescein isothiocyanate (FITC) is widely used (Seibert *et al.*, 1978). It was reported that pectins and cellulose degrading enzymes were of great importance both in the maceration of host plant and in the intercellular invasion by the pathogenic *Pythium* species (Nemec, 1974). Another study showed that *P. ultimum* contributed to the carrot cavity spot disease through extensive degradation of cellulose and pectins (Campion *et al.*, 1997). Recently, *P. ultimum* was found to contain genes encoding enzyme activities necessary for degrading the polysaccharides of the host plant cell wall (Lévesque *et al.*, 2010). On the other hand, the phytopathogenic oomycete damaged the cell walls of their host through mechanical penetration. It was demonstrated that the germ tubes of *P. aphanidermatum* penetrated directly through the cuticle cells of the tomato root (He *et al.*, 1992). Afterwards, it was reported that pectate lyase gene played an important role in *P. ultimum* pathogenesis (Fan, 2012). The activity of the cellulases produced by the phytopathogenic fungi and nutritional and environmental factors affecting the secretion of cellulases have also been well documented (EI-Said *et al.*, 2014). So far, very little direct evidence is available on the mode of degradation of *D. officinale* cell walls and on the microscopic characteristics of the host tissues upon *P. ultimum* infection. The cell wall of Oomycetes, including *P. ultimum*, contains cellulose (Fugelstad, 2008). Thus, it is necessary to conduct research on plant specific cellulase secreted by the phytopathogenic fungus which was different from the enzyme itself.

In this study, the plant specific cellulose labelled with FITC in *D. officinale* leaves and the morphological characteristics of the host plant in soft rot disease infected by *P. ultimum* were investigated in detail using SEM, TEM and the confocal laser-scanning microscope. The information obtained in this study should provide new insights underlying soft rot disease in *D. officinale*.

MATERIALS AND METHODS

Plant Material. – The samples of *D. officinale* infected by *P. ultimum* described in the manuscript were collected from Menghai *Dendrobium* cultivation field (21°57'36.64"N, 100°27'3.80"E) of Yunnan Branch Institute of Institute of Medicinal Plant Development, Chinese Academy of Medical Sciences & Peking Union Medical College in Xishuangbanna, Yunnan province, China. *D. officinale* tissue culture seedlings were preserved in the biotechnology research centre of Institute of Medicinal Plant Development, Chinese Academy of Medical Sciences. Morphological and molecular biological analyses were used to identify the plant material.

P. ultimum isolation and identification. – *P. ultimum* was isolated according to Koch's postulates from *D. officinale* specimens with damping-off disease from Menghai, Yunnan province (Li *et al.*, 2013). The pathogenic oomycete which was cultured on potato dextrose agar (PDA) medium, was identified based on morphological observation and an analysis of the rDNA ITS sequence (Li, 2011). The NCBI BLAST search program was used to search similar sequences from the GenBank sequence database for the 5.8S-ITS sequence for Oomycete. The GenBank accession number was KP676026.

Morphological observations of D. officinale infected by P. ultimum revealed by freehand sections under the light microscope. – A spore suspension (approximately 1×10^6 /mL spores) of *P. ultimum* was sprayed onto the leaves of the *D. officinale* seedlings in a greenhouse experiment using the methods of a previous study (Cheng *et al.*, 2010). Healthy leaves and diseased leaves infected by *P. ultimum* for 12 h and 24 h were cut into 0.5 mm thick freehand sections of leaf tissue. The sections were dipped into a 5% KOH solution, and a morphological examination was conducted with an AxioCan HRc Zeiss microscope (Zeiss, Germany).

Preparation of the semi-thin sections for microscopic observation. – Healthy and diseased *D. officinale* leaves were cut into 2-3 μm sections, fixed in 2.5% glutaraldehyde and stored in sealed glass bottles at 4°C for 6 h. The samples were then washed 6 times at 30 min intervals with 0.1M phosphate buffer (pH 6.8) at intervals of 30 min and subsequently fixed in 1% osmium tetroxide for 24 h at 4°C. After fixation, the samples were dehydrated in an ethanol series from 30% to 100% for 30 min and then embedded in the LR white resin. The samples were then polymerised for 48 h and cut using a diamond knife. The semi-thin sections were collected on glass slides for both microscopic observation and cytochemical staining. After staining with toluidine blue, diseased *D. officinale* leaves infected by *P. ultimum* for 12 h, 24 h and 48 h were observed using an AxioCan HRc Zeiss microscope (Zeiss, Germany).

Morphological characteristics of D. officinale infected by P. ultimum revealed by SEM. – Samples of the healthy and diseased *D. officinale* leaf tissues infected by *P. ultimum* for 12 h, 24 h and 48 h were fixed in 2.5% glutaraldehyde for 48 h at 4°C. Subsequently, the samples were air-dried and sputtered-coated with gold palladium and observed using a JEOL JSM-6510 Scanning Electron Microscope (Tokyo, Japan) (Xing *et al.*, 2013a).

Preparation of ultrathin sections for observation with TEM. – The healthy and diseased *D. officinale* leaf tissues infected by *P. ultimum* for 48 h were cut into portions of 1 mm³ in volume to prepare ultra-thin sections. The successive fixation, cleaning, post-fixation, dehydration with different concentrations of ethanol, embedding, polymerisation and cutting were performed as described above for the

semi-thin sections (Xing *et al.*, 2013b). The ultrathin sections were then collected from the nickel nets. After staining with uranyl acetate and lead citrate, the sample sections were visualised using a JEM-1400 Transmission Electron Microscope (Tokyo, Japan).

Cytochemical staining of cellulose-FITC with D. officinale leaf tissue in semi-thin sections. – The cellulase (Sigma, C8546) used in this experiment was specific to the plant. According to the protocol described previously (Seibert *et al.*, 1978), the cellulase was first conjugated with FITC, and cellulose as a substrate will then react with cellulase-FITC conjugate. The application of cellulase-FITC complex (5 mg/ml) was performed by Beijing Bioss Biotechnological Corporation with a modification of the method previously published (Benjaminson *et al.*, 1970). Briefly, 100 mg of cellulase and 2 mg FITC were dissolved in sterile Tris Buffer (0.05M, pH 9.0). The solution was stirred for 18 h at 10°C, 32,000 ×g for 30 min to remove the sediment. The supernate was dialyzed against distilled water for 48 h. Residual dye was removed by a Sephadex column. The conjugate was then frozen and dehydrated in a vacuum freeze-drying apparatus. The lyophilised powder was stored at –20°C before use.

The semi-thin sections of the healthy and the diseased leaf tissues infected by the pathogen for 12 h, and the pathogen group of *P. ultimum* without the host plant, which had been growing on PDA for 48 h. The semi-thin sections were all washed twice with 50 mM citrate buffer. Three drops of 1% BSA were added. The preparations were sealed with 0.5% gelatin for 30 min and then washed three times with double distilled water. A total of 1 ml of 0.5 mg/ml cellulose-FITC diluted with 50 mM citrate buffer solution was placed on the surfaces of the samples and incubated for 30 mins. A total of 1 ml of 50 mM citrate buffer was then added. Two washings with double distilled water were performed. The samples were naturally air-dried. The samples labelled with cellulose-FITC were then examined. The *D. officinale* mesophyll parenchyma cells from each sample were examined under a confocal laser-scanning microscope (Ultra UIEW Vox, America).

Fluorescence intensity of and data analysis of the labelled cellulose-FITC complex. – Five points were randomly selected from each 500- μm^2 -square for examination. A total of 50 images for each treatment were analysed. The mean fluorescence intensity of the healthy and diseased tissues were calculated and quantified as gray values using AxioVision Rel 4.6. The data were analysed with a t-test. All statistical analyses were performed using SPSS 11.0 (SPSS, Chicago, IL, USA). The data were presented as the means \pm SD from at least three independent experiments. *p* values <0.05 were considered significant.

RESULTS

Observation of *D. officinale* with and without *P. ultimum* infection using free-hand sections

In the healthy *D. officinale*, the leaf tissue remained intact, and the mesophyll cells were thick (Fig. 1a) and the green chloroplasts were in good order (Fig. 1a, white arrow). First, the mycelium (Fig. 1b*) of *P. ultimum* swelled and adhered to the epidermis of the leaf tissue. Then, a sporangium (Fig. 1b, right arrow) was then produced. The mycelium penetrated the cuticle of the *D. officinale* leaves and



Fig. 1. Observation of *D. officinale* with and without *P. ultimum* infection in free-hand sections. **a.** Healthy, intact *D. officinale* leaf tissues with chloroplasts in order. **b.** A sporangium (right arrow) with penetration peg (lower arrow) after infection for 12 h. **c.** Lots of *P. ultimum* mycelia and sporangia in situ after infection for 24 h, with chloroplasts distributed in disorder. Scale bars: a, b, c: 10 μ m.

temporarily colonised between the cuticle (left arrow) and the cell wall (Fig. 1b, upper arrow) 12 h after *P. ultimum* infection. The cell wall at the pathogen-infected site was compressed and deformed (Fig. 1b). A penetration peg was observed under the sporangium (Fig. 1b, lower arrow). Subsequently, the *D. officinale* leaf tissue infected by *P. ultimum* exhibited numerous *P. ultimum* mycelia (Fig. 1c, lower arrow) and sporangia (Fig. 1c, upper arrow) in the leaf tissue, and the mycelia of the pathogenic oomycete grew vigorously, with many vesicles inside the mycelia and the sporangia after 24 h of *P. ultimum* infection. After the cell walls were destroyed, the chloroplasts were dispersed in disorder (Fig. 1c, white arrow).

Morphological characteristics of *D. officinale* infected by *P. ultimum* based on observations of semi-thin sections

After the *D. officinale* leaf tissue had been in contact with *P. ultimum* for 12 h, the sporangium of the pathogen adhered to the epidermis of the cell walls (Fig. 2a, black arrows), and the local cell walls were compressed. The mesophyll cell structures inside exhibited damage, and the gap between the mesophyll cells

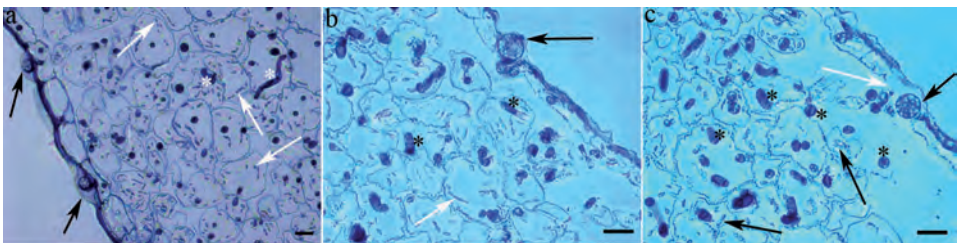


Fig. 2. Morphological characteristics of *D. officinale* infected by *P. ultimum* revealed by semi-thin sections. **a.** A sporangium adhering to the cell wall after infection for 12 h (black arrow). The chloroplasts separated from the cell membranes, resembling a string of beads (white arrows). **b.** Numerous *P. ultimum* (*) in situ 24 h after infection. The chloroplasts (white arrow) separated from the cell membrane and the sporangium (black arrow) pierced the cell wall of the epidermis. **c.** The local cell wall was broken (white arrow) 48 h after infection, with lots of *P. ultimum* mycelia (*) and the chloroplasts lined up in the cytoplasm increasingly disorderly (lower black arrows). The sporangium (upper black arrows) completely entered the mesophyll cell layer. Scale bars: a 10 μ m; b and c 20 μ m.

and the epidermis was small. Several mycelia of *P. ultimum* (Fig. 2a*) penetrated the mesophyll cell layer. The chloroplasts separated from the cell membranes and lined up in the cytoplasm, resembling a string of beads (Fig. 2a, white arrows). At 24 h after the interaction between the leaf tissue and the pathogen, the sporangium produced lots of vesicles that pierced the cell wall of the epidermis (Fig. 2b, black arrow), and the cell wall sustained additional damage. The gap between the epidermis and the mesophyll cell layer became wider, with additional mycelia in the mesophyll cell layer. The fungus in contact with the membrane of the host plant became very thin. The cell walls of the epidermis became much thinner, with the nucleus invisible and the cellular boundary obscure and incomplete (Fig. 2b). The chloroplasts (Fig. 2b, white arrow), which were smaller than the fungal mycelia (Fig. 2b*), were almost completely free from the cell membrane of the host plant. When *D. officinale* leaf tissue was infected by *P. ultimum* for 48 h, the entire sporangium entered the mesophyll cell layer from the epidermis (Fig. 2c*), the cell walls of the epidermis were effectively destroyed, and the gap between the mesophyll cell layer and the epidermis widened substantially (Fig. 2c). The cell wall of the epidermis ruptured at the site of the entrance of the pathogen (Fig. 2c, white arrow). Increasing numbers of mycelia of *P. ultimum* (Fig. 2c*) existed in the mesophyll cell layer (Fig. 2c*), and the chloroplasts increasingly formed disorderly arrangements (Fig. 2c, lower black arrows). General damage to cell structures was also observed. These pathogens (Fig. 2a*; Fig. 2b*; Fig. 2c*) were larger in size than the chloroplasts (Fig. 2a, white arrows; Fig. 2b, white arrow; Fig. 2c, black arrows).

Observation of cellulose-FITC during *P. ultimum* infection

After the cellulose of the healthy *D. officinale* mesophyll parenchyma cells was specifically marked with FITC, FITC was widely deposited in the cell walls, and the fluorescence intensity was very high (Fig. 3a). This strong fluorescence indicated that the cell structures retained their integrity and that the cellulose of *D. officinale* mesophyll parenchyma cell walls was undamaged. The chloroplasts exhibited a round or elliptical shape and were embedded in the cell membranes. However, in the specimens infected with *P. ultimum* for 12 h, the fluorescence intensity of the cellulase marked with FITC was much weaker, discontinuous and more dispersed (Fig. 3b) than that of the healthy specimens. This observation, indicated that the cell walls of the *D. officinale* mesophyll parenchyma were seriously

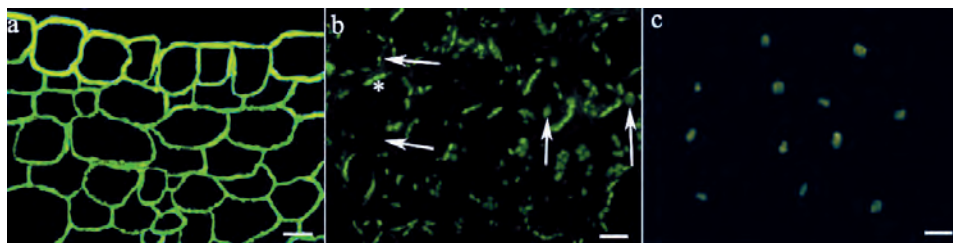


Fig. 3. Fluorescence intensity of cellulose-FITC during *P. ultimum* infection. **a.** Fluorescence intensity was very strong in healthy *D. officinale*. **b.** Fluorescence intensity was much weaker, discontinuous and dispersed in diseased *D. officinale* infected by *P. ultimum* for 12 h. **c.** The fluorescence intensity was weak in *P. ultimum* without host plant. Scale bars: a, b and c: 20 μ m.

damaged (Fig. 3b, left arrows). The chloroplasts entered the cell plasma and became distant from the cell membranes (Fig. 3b*). *P. ultimum* could only be faintly seen and was located among the mesophyll parenchyma cells (Fig. 3b, right arrows). In the pathogen group without the host plant, spherical or ovoid *P. ultimum* showed slightly greenish and could be unclearly observed (Fig. 3c).

Fluorescence intensity of the cellulose before and after *P. ultimum* infection

The fluorescence intensity of the cellulose differed significantly between the healthy and the diseased *D. officinale* mesophyll parenchyma cells ($p < 0.05$, Table 1).

Table 1. Comparison of the fluorescence intensity of the cellulose-FITC in healthy and diseased leaf tissue

Group (n=50)	Healthy leaf (control)	Diseased leaf
Fluorescence intensity	981.23 ± 46.42	235.48 ± 15.68*

The data were analysed with a t-test. The values are presented as the means ± SD from at least three independent experiments, with 50 replicates in each group. * $p < 0.05$ (compared to the control group).

SEM observations of the morphological characteristics of *D. officinale* infected by *P. ultimum*

On the abaxial surface of healthy *D. officinale*, the epidermal structure was normal, with a smooth surface and numerous guard cells (Fig. 4a, arrow). On the surface of *D. officinale* leaves without pathogen infection, the epidermis was smooth with few guard cells (Fig. 4b). After the *D. officinale* leaf tissues were infected by the pathogen for 48 h, *P. ultimum* penetrated the leaf tissue through the stomata of the guard cells (Fig. 4c, black*), and the lower hyphae became narrow and slim and changed into structures resembling penetration pegs (Fig. 4c, arrow). The appressoria (Fig. 4c, white*; Fig. 4d, black*), hemispherical in shape, grew from the germ tubes (Fig. 4c GT) and were observed at the other side of the epidermis of the leaf. The local area became inflated after 24 h of infection (Fig. 4d, arrow). *P. ultimum* mycelia penetrated the *D. officinale* leaf surface after 12 h of infection (Fig. 4e, arrows). The appressorium (Fig. 4f*) adhered to the stoma, and segmental constrictions (Fig. 4f, arrows) appeared in the *P. ultimum* mycelium.

TEM observations of *D. officinale* infected by *P. ultimum*

In the mesophyll parenchyma cells without *P. ultimum*, the cell walls and the cell structures were normal, with many chloroplasts (Fig. 5a and b, arrows) embedded in the cell membranes. After *P. ultimum* infection for 48 h, the pathogen sporangia were observed to penetrate the intercellular spaces (Fig. 5c, black arrows). New mycelia gradually developed (Fig. 5c and e, white arrow). Black deposits were distributed unevenly on the cell wall (Fig. 5c, white asterisks). The chloroplasts separated from the cell membrane and dissociated in the cytoplasm (Fig. 5c, black

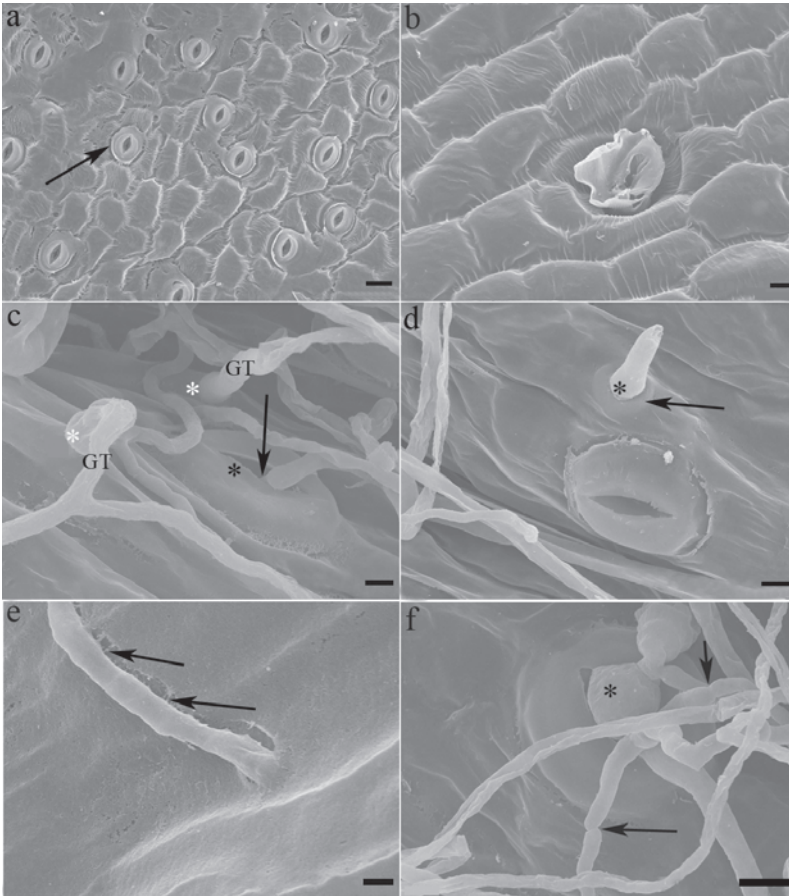


Fig. 4. Morphology of *D. officinale* infected by *P. ultimum* observed with SEM. **a.** The epidermal structure was normal on the abaxial surface of the healthy *D. officinale* with many guard cells (arrow). **b.** The epidermal structure was smooth on the surface of the healthy *D. officinale* with few guard cells. **c.** *P. ultimum* penetrated the stomata (black*) with penetration peg-like structures (arrow) and appressorium (white*) grew from the germ tubes (GT) after 48 h of infection. **d.** The appressorium (black*) formed and the local area began to inflate (arrow) after 24 h of infection. **e.** *P. ultimum* was penetrating the surface of the leaf tissues (arrows) after 12 h of infection. **f.** The appressorium adhered to the stoma and segmental constrictions appeared (arrows) after 48 h of infection. Scale bars: a 20 μm ; b 100 μm ; c 4 μm ; d 6 μm ; e 2 μm ; f 4 μm .

asterisk; Fig. 5e, black arrows). The cell walls were damaged, and the chloroplasts partially disappeared during *P. ultimum* infection (Fig. 5c and e). Numerous vesicles (Fig. 5d V) were observed inside the *P. ultimum* cells. Constrictions of the local host plant cell membrane (Fig. 5e*) occurred at the site where *P. ultimum* penetrated the intercellular space. Furthermore, the intercellular space (Fig. 5b and d, asterisk) was much wider after the pathogen entered *D. officinale* mesophyll parenchyma cells than it was in the healthy leaf tissues without *P. ultimum*.

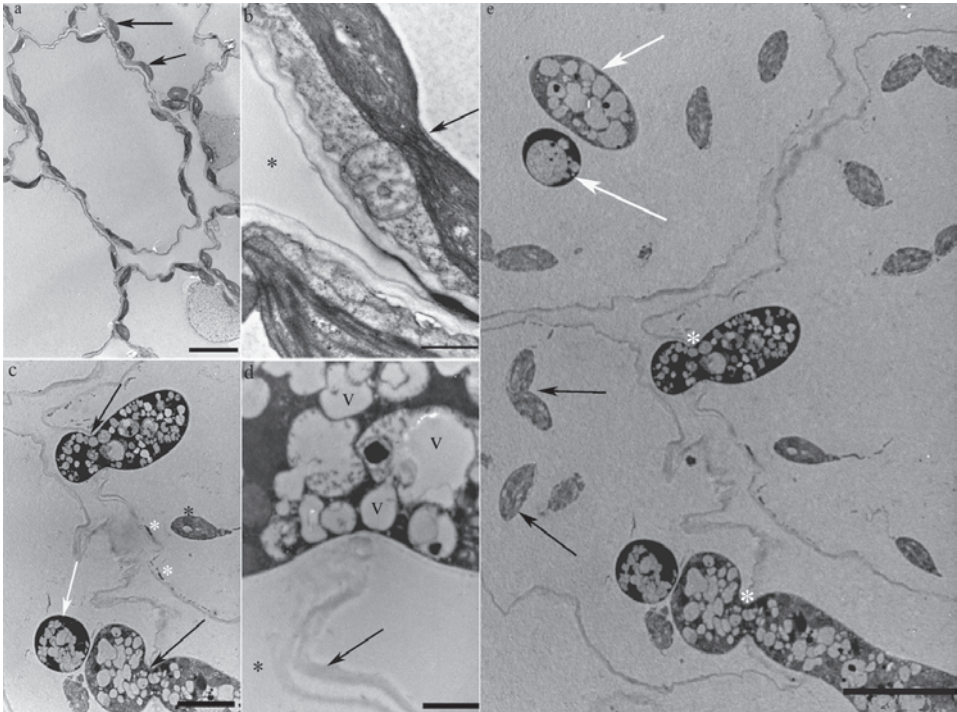


Fig. 5. TEM observations of *D. officinale* infected by *P. ultimum* after 48 h of infection. a. and b. Normal cell walls with numerous chloroplasts in healthy *D. officinale* (arrows). c. *P. ultimum* vesicles entered the intercellular spaces (black arrows). The chloroplasts separated and dissociated (black asterisk). d. The cell walls showed partial damages, and the chloroplasts disappeared. e. Constrictions of the local host plant cell membranes were observed where *P. ultimum* was penetrating the intercellular spaces (white *). The chloroplasts were dissociated from the cell membrane (black arrows). Scale bars: a 10 μm ; b 1 μm ; c 5 μm ; d 1 μm ; e 10 μm

DISCUSSION

Pythium ultimum is a ubiquitous oomycete plant pathogen on crops and ornamental species (Lévesque *et al.*, 2010). Soft rot disease caused by *P. ultimum* is also one of the most damaging diseases to *Dendrobium* species and the dominant cause of black rot in orchids (Jones, 2002). Once the disease occurs, the death of the host plant is certain.

Phytopathogenic fungi could produce infection cushion, appressorium and haustorium during the infection process (Zheng & Wu, 2007). In *Alternaria* fungi, it was reported that they damaged the cell walls of their hosts by mechanical penetration, producing mycotoxins, and secreting the degrading enzymes, mainly including cellulases and pectinases (Kang *et al.*, 2013).

In the present study, the observations of free-hand sections showed that *P. ultimum* penetrated first the cuticle, then the cell wall, and then entered the mesophyll cells of the leaves in a step-by-step manner (Fig. 1). The SEM observations

showed that the pathogen infected the host plant through the stroma or through the other side of the surface of the leaf and formed a penetration peg (Fig. 4). The chloroplasts adhered to the healthy leaves, but entered the cytoplasm upon the destruction of the cell wall of *D. officinale* (Fig. 3 and 5).

It has been reported that *Magnaporthe grisea* can produce appressoria that adhere tightly to the surface of the host and form infection pegs that serve to penetrate the underlying cell wall structures (Howard *et al.*, 1991). In most fungi, the appressorium is the most important infection structure used in host colonisation (Hoch & Staples, 1987). In *P. ultimum*, we also found that an appressorium was commonly observed during the infection of *D. officinale* leaves.

New evidence is provided regarding the mode of action of the fungus and the reaction of the plant during the early stages of fungal invasion. The results of cytochemically FITC-labeled cellulose experiment show that *P. ultimum* degrades cellulose of the plant. Cellulose in the cell walls, is progressively digested and fragmented during infection by the pathogenic fungus (Fig 3). In the process of infection, *P. ultimum* secretes enzymes to degrade the cellulose in the cell walls. After the cellulose of the host plant is degraded, the disease induced by the pathogenic fungus would spread easily. When we added excessive carboxymethyl cellulose to the reaction solution, and the cellulose was coupled with FITC and incubated with the *D. officinale* tissue, no fluorescent images appeared in the semi-thin sections (data not shown).

In the present study, the cellulase of 1,4-(1,3:1,4)- β -D-glucan 4-glucanohydrolase probe was used. This result directly demonstrated that the cellulase-FITC was more specific to the plant cellulose (Fig. 3a) than to the pathogen's cellulose (Fig. 3b and Fig. 3c), because the specific conjugate-substrate complex fluoresced a brilliant green (Seibert *et al.*, 1978). In Fig. 3c, the pathogen showed slightly greenish, which might be autofluorescence of the fungus (Seibert *et al.*, 1978). The fluorescence intensity of the fungus was weak (Fig. 3b, right arrows; Fig. 3c), which implied that the cellulose in the cell walls of *P. ultimum* was less specific to the cellulase probe. However, different from our present study, very low levels of cellulose were detected in the primary cell walls of the healthy carrot root tissues, probably due to the fact that cellulose chains did not display numerous affinity sites for the exoglucanase-gold probe (Campion *et al.*, 1998). However, β -1,4-glucans were detected over cell walls of *P. ultimum* and *P. violae* (Campion *et al.*, 1998). Thus, the inconsistency of the results with ours might be related to the application of different kinds of cellulases.

It was reported that the cellulosic glucans detected in *P. ultimum* cell walls were not altered during the host wall penetration by the oomycete. The enzymes produced by the oomycete were obviously unable to hydrolyse the cell walls of the pathogen itself (Chérif *et al.*, 1991). In our present study, the fluorescence intensity of *P. ultimum* remained unchanged when comparing before and after its interaction with the host plant (Fig. 3b, right arrows; Fig. 3c).

Among the enzymes degrading cell-wall polysaccharides, only pectate lyases and cellulases were produced by *P. violae* late and in small amounts: the symptoms caused by *P. violae* were limited and typical of cavity spot. However, *P. ultimum* secreted polygalacturonases and β -1,4-glucanases earlier and in larger amounts than *P. violae* and caused maceration of tissues, and *P. ultimum* also produced a large diversity of proteins and cellulase isoenzymes (Campion *et al.*, 1997).

Controversially, it was well documented that in *P. ultimum*, the putative cellulases belonged to families GH5, GH6 and GH7. All six GH6 candidate cellulases

harbored secretion signals. Only one GH6 protein contained a CBEL domain at the carboxyl terminus. Three possessed a transmembrane domain and one contained a glycosylphosphatidylinositol anchor, these features suggesting that these proteins might be targeting the oomycete cell wall rather than plant cell walls. The *P. ultimum* strain studied here could not grow when cellulose was the sole carbon source (Lévesque *et al.*, 2010).

The disease caused by the Oomycete pathogen in the host plant is a complex, multi-stage process, with hydrolytic enzymes, toxic metabolites (Chérif *et al.*, 1991) or a complex repertoire of effector proteins involving in pathogenesis (Liu *et al.*, 2014; Lévesque *et al.*, 2010). In order to discover which cellulases are specific to the host plant or to the pathogen, further studies such as microscopic observations combined with the use of different specific probes and analysis of the mode of degradation by *P. ultimum* should be performed. Furthermore, additional studies will also be conducted to investigate the cellulose degrading gene expression between the normal and the infected leaf tissues using quantitative real-time PCR assay later.

Acknowledgment. The research was supported by the Program for Innovation Research Team in IMPLAD (PIRTI) (IT1302) and the Doctoral Fund of Ministry of Education (20131106130002). We would like to thank Yun-Qiang Wang for samples collection. We would also like to thank Prof. Min-Woong Lee, Tae-Soo Lee and Youn-Su Lee for good suggestions in revising the manuscript.

REFERENCES

- BENJAMINSON M.A., HUNTER D.B., KATZ I.J. & SATRIANO N.M., 1970 — Purified fluorescent enzymes: preparation of large batch quantities. *Analytical Biochemistry* 34: 298-300.
- CAMPION C., MASSIOT P. & ROUXEL F., 1997 — Aggressiveness and production of cell-wall degrading enzymes by *Pythium violae*, *Pythium sulcatum* and *Pythium ultimum*, responsible for cavity spot on carrots. *European Journal of Plant Pathology* 103: 725-735.
- CAMPION C., VIAN B., NICOLE M. & ROUXEL F., 1998 — A comparative study of carrot root tissue colonization and cell wall degradation by *Pythium violae* and *Pythium ultimum*, two pathogens responsible for cavity spot. *Canadian Journal of Microbiology* 44: 221-230.
- CHENG X.L., CHENG Z.H., ZOU Y. & NIU Q., 2010 — Screen of evaluation methodology of Garlic resistance to tip blight (in Chinese). *Journal of Huazhong Agricultural University* 29: 26-30.
- CHÉRIF M., BENHAMOU N. & BÉLANGER R.R., 1991 — Ultrastructural and cytochemical studies of fungal development and host reactions in cucumber plants infected by *Pythium ultimum*. *Physiological and Molecular Plant Pathology* 39: 353-375.
- EI-SAID A.H.M., SALEEM A., MAGHRABY T.A. & HUSSEIN M.A., 2014 — Cellulase activity of some phytopathogenic fungi isolated from diseased leaves of broad bean. *Archives of Phytopathology And Plant Protection* 47(17): 2078-2094.
- FAN F.F., 2012 — Prokaryotic Expression of Pectate Lyase Gene and Pathogenic Detection of *Pythium ultimum*. *Master Degree Thesis, Jilin University*: 1-64.
- FUGELSTAD J., 2008 — Cellulose biosynthesis in Oomycetes. Licentiate Thesis in Biotechnology Stockholm, *TRITA-BIO Report* 13: 1-46.
- HE S.S., ZHANG B.X. & GE Q.X., 1992 — On the infection process of zoospores of *Pythium aphanidermatum* to tomato and Begonia (in Chinese). *Acta Phytopathologia Sinica* 22(2): 145-149.
- HOCH H.C. & STAPLES R.C., 1987 — Structural and chemical changes among the rust fungi during appressorium development. *Annual Review of Phytopathology* 25: 231-247.
- HOWARD R.J., FERRARI M.A., ROACH D.H. & MONEY N.P., 1991 — Penetration of hard substrates by a fungus employing enormous turgor pressures. *Proceedings of the National Academy of Sciences of the United States of America* 88: 11281-11284.
- JONES S., 2002 — Black rot. *Orchids* October issue: 932-933.

- KANG Z.T., JIANG L.M., LUO Y.Y., LIU C.J. & LI X.R., 2013 — The research advances of mechanism of pathogenicity of *Alternaria* phytopathogenic fungi (in Chinese). *Chinese Bulletin of Life Sciences* 25(9): 908-914.
- KIM S.J., LEE C.M., HAN B.R., KIM M.Y., YEO Y.S., YOON S.H., KOO B.S. & JUN H.K., 2008 — Characterization of a gene encoding cellulase from uncultured soil bacteria. *FEMS Microbiology Letters*: 282: 44-51.
- KLYOSOVA.A., 1990 — Trends in biochemistry and enzymology of cellulose degradation. *Biochemistry*. 29: 10577-10585.
- LÉVESQUE C.A., BROUWER H., CANO L., HAMILTON J.P., HOLT C. *et al.*, 2010 — Genome sequence of the necrotrophic plant pathogen *Pythium ultimum* reveals original pathogenicity mechanisms and effector repertoire. *Genome Biology* 11: R73.
- LI X.D., 2011 — Studies on the pathogens and control of damping-off and soft rot on *Dendrobium nobile* and *Dendrobium candidum* (in Chinese). *Ph.D. Thesis*, Chinese Academy of Medical Sciences & Peking Union Medical College: 125-130.
- LI X.D., WANG Y.Q., WANG H. & GUO S.X., 2011 — Isolation and identification of pathogen of *Dendrobium nobile* and *Dendrobium candidum* damping-off disease (in Chinese). *Chinese Pharmaceutical Journal* 46: 249-252.
- LI X.D., WANG Y.Q., WANG H. & GUO S.X., 2013 — Biocontrol of *Dendrobium candidum* damping-off disease with endophytic fungi (in Chinese). *Chinese Pharmaceutical Journal* 48: 54-58.
- LIU T.L., SONG T.Q., ZHANG X., YUAN H.B., SU L.M. *et al.*, 2014 — Unconventionally secreted effectors of two filamentous pathogens target plant salicylate biosynthesis. *Nature Communications* 5:4686.
- NEMEC S., 1974 — Production of pectinases and cellulase by six *Pythium* species isolated from necrotic strawberry roots. *Mycopathologia* 52(3-4): 283-289.
- SEIBERT G.R., BENJAMINSON M.A. & HOFFMAN H.A., 1978 — Conjugate of cellulase with fluorescein isothiocyanate: a specific stain for cellulose. *Stain Technology* 53: 103-106.
- SOMERVILLE C., 2006 — Cellulose synthesis in higher plants. *Annual Review of Cell And Developmental Biology* 22: 53-78.
- TAO Y.H., ZENG F., HO H.N., WEI J.G., WU Y.X., YANG L.L. & HE Y.Q., 2011 — *Pythium vexans* causing stem rot of *Dendrobium* in Yunan Province, China. *Journal of Phytopathology* 159: 255-259.
- XING Y.M., CHEN J., CUI J.L., CHEN X.M. & GUO S.X., 2011 — Antimicrobial activity and biodiversity of endophytic fungi in *Dendrobium devonianum* and *Dendrobium thyrsiflorum* from Vietman. *Current Microbiology* 62: 1218-1224.
- XING Y.M., CHEN J., SONG C., LIU Y.Y., GUO S.X. & WANG C.L., 2013b — Nox gene expression and cytochemical localization of hydrogen peroxide in *Polyporus umbellatus* sclerotial formation. *International Journal Molecular Sciences* 14: 22967-22981.
- XING Y.M., ZHANG L.C., LIANG H.Q., LV J., SONG C., LEE T.S. & LEE M.W., 2013a — Sclerotial formation of *Polyporus umbellatus* by low temperature treatment under artificial conditions. *PLoS One* 8: e56190.
- ZHANG L.C., CHEN J., LV Y.L., GAO C. & GUO S.X., 2012 — *Mycena* sp., a mycorrhizal fungus of the orchid *Dendrobium officinale*. *Mycological Progress* 11: 395-401.
- ZHENG L. & WU X.Q., 2007 — Advances on infection structures of plant pathogenic fungi (in Chinese). *Journal of Nanjing Forestry University (Natural Sciences Edition)* 31(1): 90-94.